Canadian Conference - Pacific Conference on Earthquake Engineering 2023
Vancouver, British Columbia
June 25th – June 30th, 2023

Implicit Coupling Using Asynchronous Time-schemes Based on Velocity Continuity at the Subdomain Interface for Seismic Engineering Problems

Stéphane Grange[1*] and David Bertrand[2]

[1]Professor, Univ. Lyon, INSA-Lyon, GEOMAS, F-69621 Villeurbanne cedex, France
[2]Assistant Professor, Univ. Lyon, INSA-Lyon, GEOMAS, F-69621 Villeurbanne cedex, France
[*]stephane.grange@insa-lyon.fr (Corresponding Author)

ABSTRACT

Seismic engineering requires to perform numerical simulations mixing phenomena having different size scales in length but also in time. For example, soil-structure interaction problems may require to assemble subdomains with very different size scales (soil, foundation and structure). Other non-smooth dynamic problems such as building poundings, rocking elements may present impacts (short time scale) during an earthquake (long time scale). Then, in order to optimise the simulations, it can be interesting to use different time integrators and spatial coupling of domains with possibly different time steps. In this work, a coupling algorithm based on a velocity continuity at the interface between two subdomains is proposed. It can take into account both heterogeneous (different time schemes) and asynchronous (different time steps) time integrations (HATI) in an implicit way. It is not intrusive in the finite element code because it can be treated as an interface element. This algorithm allows to compute efficiently the tangent algorithmic operator to keep a quadratic convergence of the simulations. Two dynamic non linear case studies are presented in this work: (1) a building pounding simulation where the part of the structure experiencing the impact is solved with the Euler+θ time integration scheme linked to the other part solved with a Newmark time integration scheme, and (2): a 2D dynamic three points bending test with J2-plasticity linking 2 subdomains (with different time schemes and time steps). All the simulations show that there is no energy dissipation at the interface and that results from this algorithm overlap very closely the reference solutions. The algorithm is therefore also generally suitable for the use of macro-elements with different internal resolution time schemes from the global solver.

Keywords: Primal subdomain coupling based on velocity continuity, Asynchronous, Time integration schemes, Implicit, Non-linear analysis.

INTRODUCTION

This work aims at coupling finite element subdomains which are not necessary treated with the same time integration schemes. Indeed, it can be interesting to consider different time integration schemes in each subdomains to account for a particular physics. For instance, for impacts problems, the adjacent zone to the impact and the rest of the structure can be solved with two different intergration schemes to account for, on the hand side, complex phenomena at the impact scale and on the other side, catch the overall response of the structure in the same modelling approach. More generally, macro-elements with internal degrees of freedom (using an internal dynamic equilibrium) can be considered. In the past years, different techniques have been developed, based on different approaches : explicit/implicit methods,[1-2], implicit/implicit through interpolation and extrapolation techniques at the interface [3], or the so-called dual method (FETI) which involves Lagrange multipliers by considering two subdomains treated at the same numerical level [4-8].

In this work, a primal method [9] is proposed which considers a subdomain 1 (master or global subdomain) calling a subdomain 2 (as a macro-element with a sub-structured resolution). Some previous work considers acceleration continuity at the interface for explicit/explicit couplings [10-11]. In this work the proposed coupling make an assumption of velocity continuity at the interface and allows to link subdomains with an implicit resolution. However, in order to compute implicit problems and to keep a quadratic convergence, this requires the correct evaluation of the algorithmic tangent operator, which will be detailed in the following (and in [12]). Finally, two non linear dynamic numerical applications are presented. The first one simulate the effects of building pounding under earthquake loading. It allows to take into account an impact in a specific zone of a structure

(described by a domain) using a complementarity method combined with an Euler integration scheme while the other part of the structure (the second domain) is solved classicaly with a Newmark time integration scheme. The second numerical application concerns the dynamic analysis of an elastoplastic beam subjected to an instantaneous force (*i.e.* problem of loss of bearing capacity). A zone of the beam is then solved with an integration scheme whose time step is m=5 times finer than the rest of the structure.

PRIMAL SUBDOMAIN AND SUB-STRUCTURING METHOD DECOMPOSITIONS

The objective is to kinematically link two subdomains (Figure 1) respecting their dynamic equilibrium (more detailed in [12]). Subdomain 1 can be seen as master part while subdomain 2 is a called by subdomain 1 as a macro-element with internal degrees of freedom and internal dynamic equilibirum. The links at the interface can be seen as boundary conditions imposed to subdomain 2 which in turn generate resisting forces applied to subdomain 1. To achieve quadratic convergence, it is necessary that subdomain 2 also returns a condensed tangent algorithmic operator at the interface with subdomain 1. When the problem is static, this type of usual static condensation is called Schur complement evaluation. In the dynamic case, with different integration schemes (heterogenous) and different time steps (asynchronous), this condensation is different and is presented below.

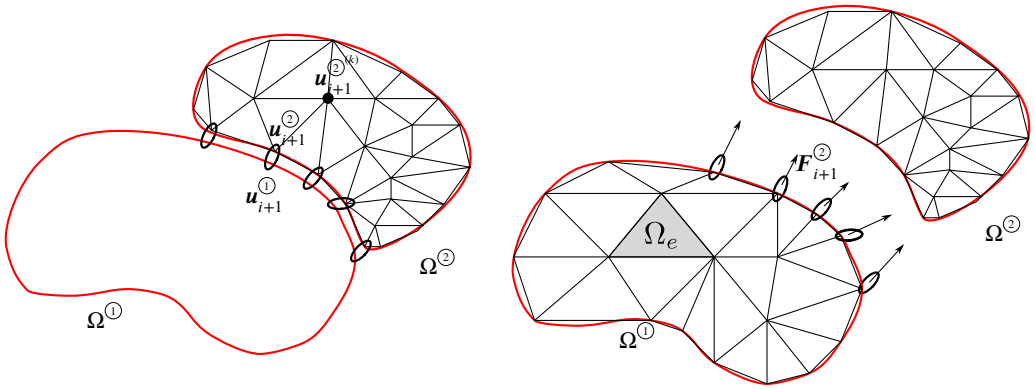

Figure 1. Representation of the decomposition of the subdomains with links at the interface. The kinematic applied at the interface (displacement, velocity and acceleration) is imposed by considering continuity of the velocities and generate resisting forces on subdomain 1 as seen in detailed in [12].

The leading idea to connect both subdomains is to impose a specific kinematic constraint at their interface in order to calculate the resisting force. In this method, and as it has been proposed for numerous FETI methods [4], it is the velocity which is chosen to be continous at the interface of both subdomains at each time step. It means the velocity is exacly the same at the interface scale for both subdomains.

In a very general way, the integration schemes allow to link displacements, velocities and possibly accelerations by means of Eq. (1) with particular parameters depending on integration schemes formulation (Newmark's family schemes, or Euler+θ scheme or Central Differences scheme recalled in Table 1).

$$\begin{cases} v^{(1)}_{i+1} = C^{(1)} u^{(1)}_{i+1} + D^{(1)}_i \\ a^{(1)}_{i+1} = A^{(1)} u^{(1)}_{i+1} + B^{(1)}_i \end{cases} \quad \text{and} \quad \begin{cases} v^{(2)}_{i+1} = C^{(2)} u^{(2)}_{i+1} + D^{(2)}_i \\ a^{(2)}_{i+1} = A^{(2)} u^{(2)}_{i+1} + B^{(2)}_i \end{cases} \tag{1}$$

Table 1. Parameters for Newmark, Euler+θ and central differences time schemes

Time scheme ⓜ	Constants	
	Coefficients	**History from previous step**
Newmark	$A^{ⓜ} = \frac{1}{\beta_m \Delta t_m^2}$ $C^{ⓜ} = \frac{\gamma_m}{\beta_m \Delta t_m}$	$B_i^{ⓜ} = -\frac{1}{\beta_m \Delta t_m^2}\left[u_i^{ⓜ} + \Delta t_m v_i^{ⓜ} + (\frac{1}{2} - \beta_m)\Delta t_m^2 a_i^{ⓜ}\right]$ $D_i^{ⓜ} = -\frac{\gamma_m}{\beta_m \Delta t_m} u_i^{ⓜ} + (1 - \frac{\gamma_m}{\beta_m}) v_i^{ⓜ} + (1 - \frac{\gamma_m}{2\beta_m})\Delta t_m a_i^{ⓜ}$
Central diff.	$A^{ⓜ} = \frac{1}{\Delta t_m^2}$ $C^{ⓜ} = \frac{2}{\Delta t_m}$	$B_i^{ⓜ} = -\frac{1}{\Delta t_m^2}\left[u_i^{ⓜ} + \frac{\Delta t_m}{2}(v_i^{ⓜ} - v_{i-1}^{ⓜ})\right]$ $D_i^{ⓜ} = -\frac{2}{\Delta t_m} u_i^{ⓜ} - v_i^{ⓜ}$
Euler+θ	$A^{ⓜ} : \{\}$ $C^{ⓜ} = \frac{1}{\theta_m \Delta t_m}$	$B_i^{ⓜ} : \{\}$ $D_i^{ⓜ} = -\frac{1}{\theta_m \Delta t_m}\left[u_i^{ⓜ} + \Delta t_m \left(1 - \theta_m\right) v_i^{ⓜ}\right]$

If the velocity is imposed to be continous at the interface, it is not possible to impose equally the displacements or accelerations at the interface. In other words, imposing velocity continuity means finding a relation between displacements on the one hand and accelerations on the other hand at the interface which involve the parameters of the 2 integration schemes. An example of this kind of link is given for the displacement in Eq. (2).

$$\boldsymbol{v}_{i+1}^{①} = \boldsymbol{v}_{i+1}^{②} \Leftrightarrow C^{①}\boldsymbol{u}_{i+1}^{①} + \boldsymbol{D}_i^{①} = C^{②}\boldsymbol{u}_{i+1}^{②} + \boldsymbol{D}_i^{②} \tag{2}$$

Finally the kinematics in terms of velocity continuity and the corrected displacement and accelerations are imposed at the interface. In addition, the condensed algorithmic tangent operator at the interface will also take into account the parameters of the two time integration schemes as it will be detailed hereafter.

Coupling of two subdomains with different time schemes having the same time step

When the two subdomains use different time schemes and with the same time step, the computation of the resisting forces of the subdomain 2 on the subdomain 1 at the interface can be seen as the results of simple boundary conditions applied to subdomain 2. The resisting force defined on all the nodes of the subdomain 2 (interface and internal nodes) can be written as Eq. (3) (this is the dynamic equlibrium, written in a general non linear way of subdomain 2):

$$\boldsymbol{F}_{i+1}^{g②} = \boldsymbol{F}^{g②}\left(\boldsymbol{U}_{i+1}^{②}, \boldsymbol{V}_{i+1}^{②}, \boldsymbol{A}_{i+1}^{②}\right) \tag{3}$$

Where $\boldsymbol{U}_{i+1}^{(2)}, \boldsymbol{V}_{i+1}^{(2)}, \boldsymbol{A}_{i+1}^{(2)}$ concatenate the degrees of freedom at the boundary (b) and the internal degrees of freedom (r) as defined hereafter for the displacement. In the following, the internal degrees of freedom (r) are denoted finally with a (k) upperscript to keep in mind the internal solution of subdomain (2) can be non linear and evaluated over few iterations (k) with an incremental procedure (as Newton Raphson). For the boundary degrees of freedom (b), as the kinematic is imposed throughout the time step, the notation contains only the time step (i+1):

$$\boldsymbol{U}_{i+1}^{②} = \begin{bmatrix} \boldsymbol{u}_b \\ \boldsymbol{u}_r \end{bmatrix} = \begin{bmatrix} \boldsymbol{u}_{i+1}^{②} \\ \boldsymbol{u}_{i+1}^{②^{(k)}} \end{bmatrix} \tag{4}$$

The linearization of the force can then be written as (where $\boldsymbol{M}, \boldsymbol{C}, \boldsymbol{K}$ are the linearized operators defined in a general way here which are due to the constitutive mechanisms of the subdomain 2):

$$d\boldsymbol{F}^{g②}\left(\boldsymbol{U}_{i+1}^{②}, \boldsymbol{V}_{i+1}^{②}, \boldsymbol{A}_{i+1}^{②}\right) = \boldsymbol{M}d\boldsymbol{A}_{i+1}^{②} + \boldsymbol{C}d\boldsymbol{V}_{i+1}^{②} + \boldsymbol{K}d\boldsymbol{U}_{i+1}^{②} \tag{5}$$

This last equation can also be rewritten in block matrix form to understand the sub-structuration of the method and showing the concatenation of the degrees of freedom and resisting force at the interface (block equation 1), as well as the internal degrees of freedom and internal force (block Eq. (2)):

$$d\boldsymbol{F}^{g②} = \begin{bmatrix} d\boldsymbol{F}_{i+1}^{②} \\ d\boldsymbol{F}_{i+1}^{②^{(k)}} \end{bmatrix} = \begin{bmatrix} \boldsymbol{M}_{bb} & \boldsymbol{M}_{br} \\ \boldsymbol{M}_{rb} & \boldsymbol{M}_{rr} \end{bmatrix} \begin{bmatrix} d\boldsymbol{a}_{i+1}^{②} \\ d\boldsymbol{a}_{i+1}^{②^{(k)}} \end{bmatrix} + \begin{bmatrix} \boldsymbol{C}_{bb} & \boldsymbol{C}_{br} \\ \boldsymbol{C}_{rb} & \boldsymbol{C}_{rr} \end{bmatrix} \begin{bmatrix} d\boldsymbol{v}_{i+1}^{②} \\ d\boldsymbol{v}_{i+1}^{②^{(k)}} \end{bmatrix} + \begin{bmatrix} \boldsymbol{K}_{bb} & \boldsymbol{K}_{br} \\ \boldsymbol{K}_{rb} & \boldsymbol{K}_{rr} \end{bmatrix} \begin{bmatrix} d\boldsymbol{u}_{i+1}^{②} \\ d\boldsymbol{u}_{i+1}^{②^{(k)}} \end{bmatrix} \tag{6}$$

Using the time schemes parameters, the global equivalant stiffness matrix of subdomain 2 can be obtained as in Eq. (7) in relation with the displacement field for example using Eq. (2):

$$d\boldsymbol{F}_{i+1}^{g\,②} = \underbrace{\left(\boldsymbol{M}\boldsymbol{A}^{②} + \boldsymbol{C}\boldsymbol{C}^{②} + \boldsymbol{K}\right)}_{\tilde{\boldsymbol{K}}} d\boldsymbol{U}_{i+1}^{②} \tag{7}$$

Which can be rewritten as:

$$\begin{bmatrix} d\boldsymbol{F}_{i+1}^{②} \\ d\boldsymbol{F}_{i+1}^{②(k)} \end{bmatrix} = \tilde{\boldsymbol{K}} \begin{bmatrix} d\boldsymbol{u}_{i+1}^{②} \\ d\boldsymbol{u}_{i+1}^{②(k)} \end{bmatrix} = \tilde{\boldsymbol{K}} \begin{bmatrix} C^{②^{-1}} C^{①} d\boldsymbol{u}_{i+1}^{①} \\ d\boldsymbol{u}_{i+1}^{②(k)} \end{bmatrix} \tag{8}$$

At convergence, the internal forces (on internal degrees of freedom r) vanish:

$$\boldsymbol{F}_{i+1}^{②(k)} = -\boldsymbol{R}_{i+1}^{②(k)} = \boldsymbol{0} \tag{9}$$

This last equation allows to evaluate the schur complement (static condensation of the 2nd line into the 1st line of Eq. (8)). The relationship between the increment of forces at the interface and the increment of displacement imposed by the subdomain 1 can be then calculated and provides the algorithmic tangent operator (which depends on time schemes parameters of both subdomains):

$$d\boldsymbol{F}_{i+1}^{②} = \underbrace{\left[\tilde{\boldsymbol{K}}_{bb} - \tilde{\boldsymbol{K}}_{br}\tilde{\boldsymbol{K}}_{rr}^{-1}\tilde{\boldsymbol{K}}_{rb}\right]}_{\tilde{\boldsymbol{k}}} C^{②^{-1}} C^{①} d\boldsymbol{u}_{i+1}^{①} \tag{10}$$

Coupling of two subdomains with different time schemes and with different time steps

If the time step of subdomain 2 is smaller (time step dt_2) than the one of subdomain 1 (time step $dt_1 = m dt_2$, with $m \in N^+$), a kinematic assumption must be imposed at the interface during the whole coarse time step (dt_1) using a parameter λ_{p+1} increasing incrementally troughout the coarse time step i+1. Classicaly in FETI methods, the velocity in subdomain 2 at the interface is imposed to evolve linearly between the beginning and the end of the coarse time step as in Eq. (11) and Figure 2:

$$\boldsymbol{v}_{p+1}^{②} = \lambda_{p+1}\boldsymbol{v}_{i+1}^{①} + \lambda_p \boldsymbol{v}_i^{①} \tag{11}$$

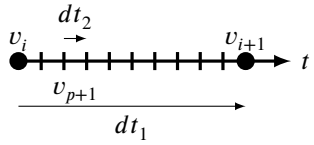

Figure 2. Finer time step decomposition of subdomain 2 into the coarse time step of subdomain 1

For every fine time step $p+1$ between i and $i+1$, the global resisting force (for all nodes) is evaluated in subdomain 2.

$$\boldsymbol{F}_{p+1}^{g②} = \begin{bmatrix} \boldsymbol{f}_b \\ \boldsymbol{f}_r \end{bmatrix} = \begin{bmatrix} \boldsymbol{F}_{p+1}^{②} \\ \boldsymbol{F}_{p+1}^{②(k)} \end{bmatrix} = \begin{bmatrix} \boldsymbol{F}_{p+1}^{②} \\ -\boldsymbol{R}_{p+1}^{(k)} \end{bmatrix} \tag{12}$$

The objective is now to calculate the differentation of the force at the interface $\boldsymbol{F}_{p+1}^{(2)}$ with the increment of displacement at the interface imposed at the interface for each fine time step dt_2 (Eq. (13)).

$$\tilde{\boldsymbol{k}}_{p+1} = \frac{\partial \boldsymbol{F}_{p+1}^{②}}{\partial \boldsymbol{u}_{i+1}^{①}} \tag{13}$$

This operator evaluated when $p+1$ corresponds to $i+1$ (*i.e.* at the end of the coarse step) will be the algoritmnic tangent operator. In order to calculate exactly this tangent operator, the resisting force vector must be differentiated (as it has been done in the previous section), but now taking into account that the variables of the previous substep p are no longer constants and must be differentiated too. It leads to Eq. (14):

$$d\boldsymbol{F}_{p+1}^{g\,②} = \underbrace{\left(\boldsymbol{M}\boldsymbol{A}^{②} + \boldsymbol{C}\boldsymbol{C}^{②} + \boldsymbol{K}\right)}_{\tilde{\boldsymbol{K}}} d\boldsymbol{U}_{p+1}^{②} + \underbrace{\left[\,\boldsymbol{M}\;\;\boldsymbol{C}\,\right]}_{\tilde{\boldsymbol{S}}} d\boldsymbol{W}_{p}^{②} \tag{14}$$

Where, the array $\boldsymbol{W}_p^{(2)}$ contains the times schemes parameters defined at the previous sub time step:

$$\boldsymbol{W}_{\boldsymbol{p}}^{②} = \begin{bmatrix} \boldsymbol{B}_{p}^{g\,②} \\ \boldsymbol{D}_{p}^{g\,②} \end{bmatrix} \tag{15}$$

Moreover, at the interface, by imposing the velocity evolving linearly during the coarse time step, a kinematic relationship can be written between the displacement at the interface in subdomain 2 and the displacement imposed at the end of the coarse time step at the interface in subdomain 1:

$$d\boldsymbol{u}_{p+1}^{②} = H_{p+1}^{②} d\boldsymbol{u}_{i+1}^{①} \tag{16}$$

With:

$$H_{p+1}^{②} = C^{②^{-1}} \lambda_{p+1} C^{①} + \sum_{j=0}^{p} {}^{t}\boldsymbol{r}_{u}^{②} \boldsymbol{m}^{②^{j}} \boldsymbol{q}^{②} H_{p-j}^{②} \tag{17}$$

With $\boldsymbol{r}_u^{(2)}$, $\boldsymbol{m}^{(2)}$ and $\boldsymbol{q}^{(2)}$, rectangular operators only dependant on the time scheme parameters of subdomain 2 (as developed in details in [12]).

The last term of Eq. (14) that must to be evaluated is the increment of kinematic array $d\boldsymbol{W}_p^{(2)}$ which can be calculated using the time scheme parameters of subdomain 2 as demonstrated in [12] and where $\boldsymbol{M}^{(2)}$ and $\boldsymbol{Q}^{(2)}$ are rectancular operators that concatenante $\boldsymbol{m}^{(2)}$ and $\boldsymbol{q}^{(2)}$ (as developed in detailed in [12])

$$d\boldsymbol{W}_{p}^{②} = \boldsymbol{M}^{②} d\boldsymbol{W}_{p-1}^{②} + \boldsymbol{Q}^{②} d\boldsymbol{U}_{p}^{②} \tag{18}$$

Finally the increment of the resisting force of subdomain 2 can be calculated over every fine time step $p+1$ of subdomain 2 and is given by Eq. (19):

$$d\boldsymbol{F}_{p+1}^{g\,②} = \tilde{\boldsymbol{K}} d\boldsymbol{U}_{p+1}^{②} + \sum_{j=0}^{p} \tilde{\boldsymbol{S}} \boldsymbol{M}^{②^{j}} \boldsymbol{Q}^{②} d\boldsymbol{U}_{p-j}^{②} \tag{19}$$

This last equation contains the resisting force at the interface (b) and for the internal nodes (r). Because at convergence, there is equilibrium on the internal degrees of freedom and then $\boldsymbol{R}_{p+1}^{(k)} = 0$ vanishes as in Eq. (12), it is then possible to condense this equation on the equations at the interface.

$$\tilde{\boldsymbol{K}}_{rb} d\boldsymbol{u}_{p+1}^{②} + \tilde{\boldsymbol{K}}_{rr} d\boldsymbol{u}_{p+1}^{②^{(k)}} + \sum_{j=0}^{p} \left[\left(\tilde{\boldsymbol{S}} \boldsymbol{M}^{②^{j}} \boldsymbol{Q}^{②} \right)_{rb} d\boldsymbol{u}_{p-j}^{②} + \left(\tilde{\boldsymbol{S}} \boldsymbol{M}^{②^{j}} \boldsymbol{Q}^{②} \right)_{rr} d\boldsymbol{u}_{p-j}^{②^{(k)}} \right] = \boldsymbol{0} \tag{20}$$

The link between $d\boldsymbol{u}_{p+1}^{(2)}$ is then introduce into the first equation of Eq. (19) (dynamic condensation):

$$\tilde{\boldsymbol{K}}_{bb} d\boldsymbol{u}_{p+1}^{②} + \tilde{\boldsymbol{K}}_{br} d\boldsymbol{u}_{p+1}^{②^{(k)}} + \sum_{j=0}^{p} \left[\left(\tilde{\boldsymbol{S}} \boldsymbol{M}^{②^{j}} \boldsymbol{Q}^{②} \right)_{bb} d\boldsymbol{u}_{p-j}^{②} + \left(\tilde{\boldsymbol{S}} \boldsymbol{M}^{②^{j}} \boldsymbol{Q}^{②} \right)_{br} d\boldsymbol{u}_{p-j}^{②^{(k)}} \right] = d\boldsymbol{F}_{p+1}^{②} \tag{21}$$

The following relationship can then be obtained :

$$\frac{\partial \boldsymbol{F}_{p+1}^{②}}{\partial \boldsymbol{u}_{i+1}^{①}} = \underbrace{\tilde{\boldsymbol{K}}_{bb} H_{p+1}^{②} + \tilde{\boldsymbol{K}}_{br} \boldsymbol{T}_{p+1} + \sum_{j=0}^{p} \left[\left(\tilde{\boldsymbol{S}} \boldsymbol{M}^{②^{j}} \boldsymbol{Q}^{②} \right)_{bb} H_{p-j}^{②} + \left(\tilde{\boldsymbol{S}} \boldsymbol{M}^{②^{j}} \boldsymbol{Q}^{②} \right)_{br} \boldsymbol{T}_{p-j} \right]}_{\tilde{\boldsymbol{k}}_{p+1}} \tag{22}$$

Finally, the computation of the algorithimic tangent operator from subdomain 2 to subdomain 1 is summarized as follows and requires only to compute rectangular operators (that only contains time schemes parameters), and is quite straightforward to calculate over the coarse time step of subdomain 1.

$$\begin{cases} H_{p+1}^{②} = C^{②^{-1}} \lambda_{p+1} C^{①} + \sum_{j=0}^{p} {}^{t}\boldsymbol{r}_{u}^{②} \boldsymbol{m}^{②^{j}} \boldsymbol{q}^{②} H_{p-j}^{②} \\ \boldsymbol{T}_{p+1} = -\tilde{\boldsymbol{K}}_{rr}^{-1} \left[\tilde{\boldsymbol{K}}_{rb} H_{p+1}^{②} + \sum_{j=0}^{p} \left[\left(\tilde{\boldsymbol{S}} \boldsymbol{M}^{②^{j}} \boldsymbol{Q}^{②} \right)_{rb} H_{p-j}^{②} + \left(\tilde{\boldsymbol{S}} \boldsymbol{M}^{②^{j}} \boldsymbol{Q}^{②} \right)_{rr} \boldsymbol{T}_{p-j} \right] \right] \\ \tilde{\boldsymbol{k}}_{p+1} = \tilde{\boldsymbol{K}}_{bb} H_{p+1}^{②} + \tilde{\boldsymbol{K}}_{br} \boldsymbol{T}_{p+1} + \sum_{j=0}^{p} \left[\left(\tilde{\boldsymbol{S}} \boldsymbol{M}^{②^{j}} \boldsymbol{Q}^{②} \right)_{bb} H_{p-j}^{②} + \left(\tilde{\boldsymbol{S}} \boldsymbol{M}^{②^{j}} \boldsymbol{Q}^{②} \right)_{br} \boldsymbol{T}_{p-j} \right] \end{cases} \tag{23}$$

The same kind of demonstration can be done when the main unknowns of subdomain 1 or 2 (or both of them) is the velocity (instead of the displacement). More details are provided and demonstrated in [12].

NUMERICAL SIMULATIONS

Building pounding (Newmark/Euler coupling)

In this section, a portal frame with a node in contact with an adjacent very stiff building is subjected to a seismic input. In order to correctly take into account the rigid contact, a linear complementarity problem [13] must be solved within the framework of non smooth mechanics. Thus, an Euler integration scheme (first order scheme) is used to correctly treat the velocity discontinuities at the time of impact. The dynamic equilibrium of domain 1 (in black on the figure) is treated with a Newmark scheme ($\beta = \frac{1}{4}, \gamma = \frac{1}{2}, dt_1 = 1.10^{-3}s$), while domain 2 (where complementarity is taken into account for the impact, see [13] for more details on this technique) is solved dynamically with an Euler+θ scheme ($\theta = \frac{1}{2}, m = \frac{dt_1}{dt_2} = 1$). The interface between both subdomains (at nodes 4 and 5) is treated using the proposed algorithm. Euler-Bernoulli beam finite elements are used with the following parameters: Young's modulus $E = 30.10^9 Pa$, cross section $S = 0.04m^2$, inertia $Iz = 3.3.10^{-5}m^4$ and a density $\rho = 2500kg/m^3$. As the contact is very rigid, a viscous damping $\eta = 5.10^{-3}$s (defined on the stiffness matrix as $\boldsymbol{C} = \eta \boldsymbol{K}$) is considered into the structure in order to attenuate the spurious vibrations. Perfect hinges are considerated as boundary conditions at nodes 1 and 2 and the impact occurs at node 6. An initial gap *g=0.2m* is considered between node 6 and the rigid contact-impact point.

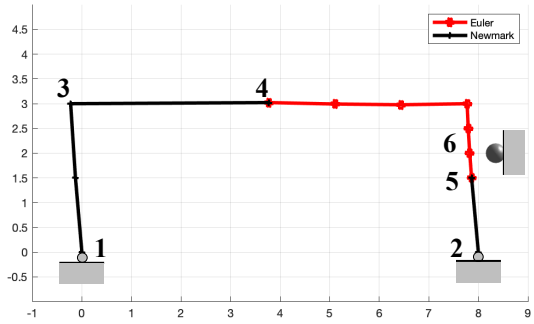

Figure 3. Portal frame under seismic loading with impact (building pounding): in black the subdomain 1 solved with a Newmark time scheme and in red the domain 2 solved using an Euler time scheme and the complementarity method for the impact.

A reference test case is also performed (using Euler time scheme for the whole structure without substructuring the problem). The Figure 4 shows a comparison of the model decomposed into 2 subdomains (named multi_TS) with the reference for $m = \frac{dt_1}{dt_2} = 1$ in terms of horizontal displacement (Figure 4(a)) and horizontal velocity (Figure 4(b)) of the node 3. The proposed interface allows to obtain very good agreement between the simulations. Figure 4(c) shows the evolution of kinematic and elastic potential energy. Total mechanical energy is also displayed (by considering the seisimic input energy and the viscous dissipation). The total energy remains constant. This means the interface element between the subdomains does not dissipate energy.

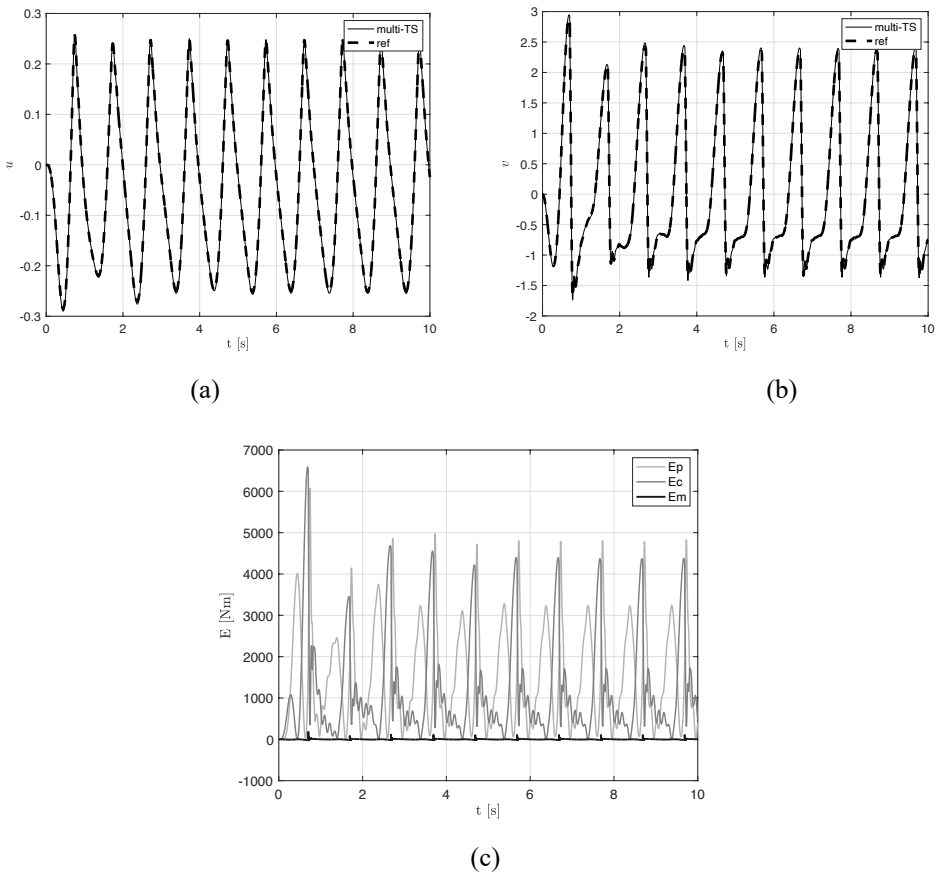

Figure 4. Portal frame under seismic loading with impact (building pounding). Comparison between the multi time schemes simulations and a reference solution: (a) horizontal displacements, (b) horizontal velocity at node 3, and (c) energy balance.

In terms of convergence, the algorithmic tangent operator provided by the interface element allows to keep a quadratic convergence of the model.

2D non linear dynamic three points bending test (Newmarl/Euler coupling)

This numerical simulation considers a 2D dynamic three points bending test. The beam (L=10.5m length, h=1m height, e=0.3m thick) is clamped at its both ends and an instantaneous vertical force is applied at mid span (Figure 5). It simulates a progressive collapse when a support at the middle of the beam is lost due to an accidental solicitation. In order to make sure the algorithm does not dissipate energy, the force $F_y = -7MN$ is then released at t=0.1s and the beam freely oscillates until the end of the simulation. Subdomain 1 is simulated with Newmark time scheme ($\beta = \frac{1}{4}, \gamma = \frac{1}{2}, dt_1 = 2.10^{-4}s$) while subdomain 2 is solved using Euler+θ method ($\theta = \frac{1}{2}, m = \frac{dt_1}{dt_2} = 5$).

A non-linear constitutive law (plane stress J2 plasticity, see Simo and Hughes [14]) is considered with a Young's modulus E = 210 GPa, a Poisson's ratio ν = 0.2, a yield stress fy = 500 MPa, an isotropic hardening parameter H = 20 GPa, and a density ρ = 7800 kg⁄m3. In this simulation, as the response of the beam is quite smooth, no damping has been considered. It means the only dissipation of energy is due to plasticity (material damping). After t=0.1s and due to hardening developed earlier, the beam oscillates in its linear domain and shows no dissipation while a permanent deflection is generated.

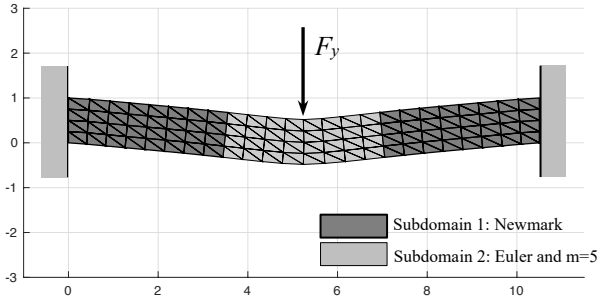

Figure 5. 2D dynamic three points bending test. The domain 1 is solved with a Newmark time scheme and in the domain 2 is solved using an Euler time scheme. An instanenous force is applied at the middle at t=0s and then released at t=0.1s.

The Figure 6 shows the displacements, velocity and energy balance. The oscillations of the beam have a constant amplitude after releasing the force and the energy remains constant showing that no energy is dissipated at the interface.

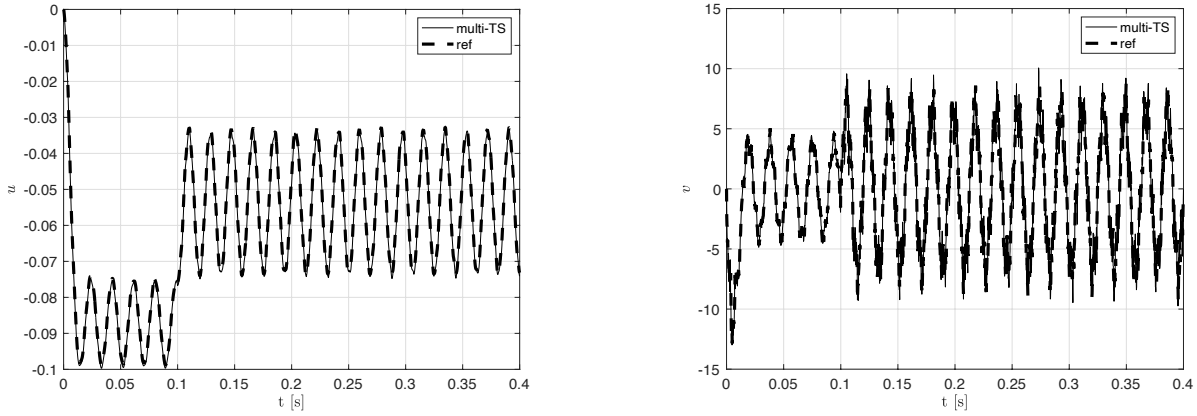

(a) *(b)*

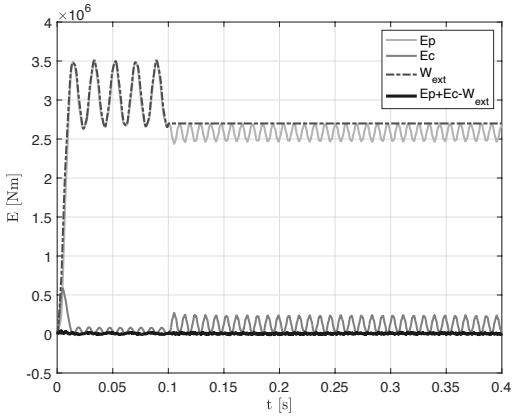

(c)

Figure 6. 2D dynamic three point bending test. Comparison between the multi time schemes simulations and a reference solution: (a) vertical displacements, (b) vertical velocity at the middle of the beam, and (c) energy balance.

CONCLUSIONS

The coupling method presented in this work allows to sub-structure domains whose resolution is implicit and with different time schemes (heteregoneous) and different time steps (asynchronous). The algorithmic tangent operator allowing to keep a quadratic convergence are demonstrated. From the examples, it is shown that there is no energy dissipation due to the resolution of the interface between the two domains. Other couplings can be considered with this method with HHT type schemes or algorithms for solving partial differential equations based on Cauchy problems.

REFERENCES

[1] Liu W, Belytschko T. Mixed-time implicit-explicit finite elements for transient analysis. Computers & Structures 1982; 15(4): 445 - 450. doi: https://doi.org/10.1016/0045-7949(82)90079-7

[2] Hughes TJR, Liu WK. Implicit-Explicit Finite Elements in Transient Analysis: Stability Theory. Journal of Applied Mechanics 1978; 45(2): 371-374. doi: 10.1115/1.3424304

[3] Belytschko T, Mullen R. Stability of explicit-implicit mesh partitions in time integration. International Journal for Numerical Methods in Engineering 1978; 12(10): 1575-1586. doi: 10.1002/nme.1620121008

[4] Combescure A, Gravouil A. A time-space multi-scale algorithm for transient structural nonlinear problems. Mécanique & Industries 2001; 2(1): 43 - 55.

[5] Avery P, Farhat C. The FETI family of domain decomposition methods for inequality-constrained quadratic programming: Application to contact problems with conforming and nonconforming interfaces. Computer Methods in Applied Mechanics and Engineering 2009; 198(21): 1673 - 1683. Advances in Simulation-Based Engineering Sciences – Honoring J. Tinsley Odendoi: https://doi.org/10.1016/j.cma.2008.12.014

[6] Beneš M, Kruis J. Multi-time-step domain decomposition and coupling methods for nonlinear parabolic prob- lems. Applied Mathematics and Computation 2018; 319: 444 - 460. Recent Advances in Computingdoi: https://doi.org/10.1016/j.amc.2017.04.026

[7] Beneš M, Krejčí T, Kruis J. A FETI-based mixed explicit-implicit multi-time-step method for parabolic problems. Journal of Computational and Applied Mathematics 2018; 333: 247 - 265. doi: https://doi.org/10.1016/j.cam.2017.10.041

[8] Brun M, Gravouil A, Combescure A, Limam A. Two FETI-based heterogeneous time step coupling methods for Newmark and α-schemes derived from the energy method. Computer Methods in Applied Mechanics and Engineering 2015; 283: 130 - 176. doi: https://doi.org/10.1016/j.cma.2014.09.010

[9] Escaig Y, Marin P. Examples of domain decomposition methods to solve non-linear problems sequentially. Advances in Engineering Software 1999; 30(9): 847 - 855. doi: https://doi.org/10.1016/S0965-9978(98)00114-8

[10] Smolinski P. An explicit multi-time step integration method for second order equations. Computer Methods in Applied Mechanics and Engineering 1992; 94(1): 25 - 34. doi: https://doi.org/10.1016/0045-7825(92)90155-D

[11] Smolinski P. Stability analysis of a multi-time step explicit integration method. Computer Methods in Applied Mechanics and Engineering 1992; 95(3): 291 - 300. doi: https://doi.org/10.1016/0045-7825(92)90188-P

[12] Grange S, Bertrand D., Implicit coupling of heterogeneous and asynchronous time-schemes using a primal approach based on velocity continuity at the subdomain interface, Finite Elements in Analysis and Design, Volume 196, 2021, 103604, ISSN 0168-874X, https://doi.org/10.1016/j.finel.2021.103604.

[13] Acary V. Projected event-capturing time-stepping schemes for nonsmooth mechanical systems with unilateral con- tact and Coulomb's friction. Computer Methods in Applied Mechanics and Engineering 2013; 256: 224 - 250. doi: https://doi.org/10.1016/j.cma.2012.12.012

[14] J. Simo, T. Hughes, Computational Inelasticity. Mechanics and Materials, vol. 7, Springer Interdisciplinary applied mathematics, 1998.